Journal of Alloys and Compounds 651 (2015) 666–672

Contents lists available at ScienceDirect

Journal of Alloys and Compounds

journal homepage: http://www.elsevier.com/locate/jalcom

Low-temperature synthesis of nanosized metal borides through reaction of lithium borohydride with metal hydroxides or oxides

Wei Yuan Pan [a], Qian Wen Bao [a], Yang Jun Mao [a], Bin Hong Liu [a, *], Zhou Peng Li [b]

[a] Dept. of Materials Sci. & Eng., Zhejiang University, Hangzhou 310027, PR China
[b] Dept. of Chemical & Biological Eng., Zhejiang University, Hangzhou 310027, PR China

ARTICLE INFO

Article history:
Received 26 July 2015
Received in revised form
17 August 2015
Accepted 18 August 2015
Available online 20 August 2015

Keywords:
Metal boride
Lithium borohydride
Hydroxide
Oxide
Nanostructure

ABSTRACT

In this study, we report a novel and facile synthesis approach of boron-rich transition metal borides such as LaB_6 and TiB_2 through reaction of lithium borohydride ($LiBH_4$) with corresponding metal hydroxide or oxide at temperatures below 600 °C. A fast endothermic reaction occurred at around 350 °C in the ball milled mixture of $6LiBH_4 + La(OH)_3$ or $12LiBH_4 + La_2O_3$, efficiently producing crystalline LaB_6 nanoparticles of a size smaller than 100 nm. In comparison, the reaction of $LiBH_4$ with TiO_2 proceeded within a wide temperature range from 120 °C to 500 °C, resulting in the formation of nanocrystalline TiB_2 of only a few nanometers. This synthesis method proved to be a facile and general route to fabricate nanosized transition metal borides.

1. Introduction

Metal borides are a group of chemicals with unique structures and properties, and thus are used in versatile applications [1,2]. For example, MB_2 (M = Mg, Al, Ti, V, Zr, Nb etc.) has a layered structure with alternating layers of metal and boron. MB_6 (M = Ca, La, Ce etc.) has a CsCl structure in which the site of Cs^+ is occupied by a metal ion, while Cl^- is replaced by a covalently bonded B_6 octahedron [1]. These boron-rich metal borides are known as refractory materials that commonly have high hardness and melting points, high resistance to wear and corrosion, high chemical stability, excellent thermal and electric conductivity [1,2]. They can thus be used in extreme environments such as for aerospace applications. In recent years, several metal borides are found to have functional properties [1–8]. For example, MgB_2 is a superconductor with a superconducting temperature of 39 K [1,2]. LaB_6 and CeB_6 are excellent field emission materials used in scanning and transmission electron microscopes [1,2]. VB_2 or TiB_2 is found with extremely high electrochemical capacities around 4500 mAh g^{-1} in a VB_2 (TiB_2)-air battery [3,4]. TiB_2 is also used as a catalyst support in proton exchange membrane fuel cell (PEMFC) [5]. Therefore, more and more metal borides are being developed as functional materials.

However, synthesis of metal borides is challenging mainly due to the lack of reactive elemental boron sources [1,2] They are usually synthesized using elemental materials of metals and boron by hot pressing, spark plasma sintering, fused salt electrolysis, self-propagating high-temperature synthesis, chemical vapor deposition, etc. Due to the very high melting point of 2075 °C and chemical inertness of elemental boron, the fabrication temperatures of metal borides are usually higher than 1100 °C [1]. High synthesis temperatures of metal borides not only lead to high energy consumption, but also induce pollution from crucible, raw materials as well as atmosphere. Moreover, metal borides prepared at high temperatures suffer from poor size control. On the other hand, nanosized powders with homogeneous composition and narrowly distributed particle size are in demand to improve their sinterability.

Considering more and more important roles played by metal borides and relatively less knowledge of their synthesis, considerable research effort is being made to develop new, facile and general synthesis routes for metal borides [9–16]. For example, a general solution route to synthesize metal boride nanocrystals has recently been developed using metal chlorides and sodium borohydrdie ($NaBH_4$) as the reactants [9]. A eutectic LiCl/KCl salt mixture was used to initiate the reaction in the liquid state. Using this synthesis process, nanocrystals of CaB_6 and NbB_2 as examples

* Corresponding author.
E-mail address: liubh@zju.edu.cn (B.H. Liu).

http://dx.doi.org/10.1016/j.jallcom.2015.08.149
0925-8388/

have been obtained under a synthesis temperature of 800–900 °C. In another research work, nano powders of TiB_2 and VB_2 have been mechanochemically synthesized by using $LiBH_4$, LiH and clorides such as $TiCl_3$ or VCl_3 [10]. Nanosized LaB_6 crystals have been fabricated at 400 °C starting from Mg powder, $NaBH_4$ and $LaCl_3$ [14].

In this study, we introduce a facile and general synthesis method of transition metal borides such as LaB_6 and TiB_2 at temperatures below 600 °C. $LiBH_4$ was used as the boron source as well as the reductive agent. It reacted with metal hydroxide such as $La(OH)_3$ or oxides such as La_2O_3 or TiO_2 to fabricate nanosized crystalline LaB_6 or TiB_2. The results shown in this study provide a new, facile and general synthesis route for nanosized and crystalline transition metal borides, thus shedding light on developments of novel synthesis approaches and performance enhancements of these metal borides.

2. Experimental details

2.1. Materials

The chemicals and raw materials used in this study were commercially purchased as follows: $LiBH_4$ (95%, Acros), $La(OH)_3$ (99.9%, Aladdin), La_2O_3 (99.99%, Aladdin), TiO_2 (99.8%, Aladdin).

2.2. Synthesis process of metal borides

The mixtures of $LiBH_4$ with $La(OH)_3$, La_2O_3 or TiO_2 in stoichiometric molar ratios were first ball milled at 400 rpm for 16 h in a planetary mill. The stainless steel vessel for ball milling was 100 ml and the weight ratio of ball to sample was 180:1. The ball milled mixture was then introduced into a stainless steel reactor. The handling of ball milling samples was undergone in a glove box filled with high purity argon gas in which the levels of H_2O and O_2 were kept below 1 ppm. The sealed reactor was then set up on a Sievert's apparatus. The reactor was first evacuated and then heated from room temperature to 600 °C at 2 °C min^{-1}. The pressure in the system was recorded during the experiments. The amount of gas release was then determined according to the pressure rise in the reactor. The final pressure in the reactor was lower than 0.15 MPa.

2.3. Instrumental characterizations and analyses

X-ray diffraction (XRD) analyses were performed on a PANalytical X'Pert PRO using the CuKα radiation. A special sample stand was designed to protect the samples from air exposure during XRD measurements. Differential Scanning Calorimetry (DSC) analyses were conducted on a Netzsch STA449F3 at a heating rate of 5 °C min^{-1} under argon atmosphere with a flow rate of 50 ml min^{-1}. Field emission scanning electron microscopy (FE-SEM) observations were carried out on a Hitachi SU-70 microscope. The samples were protected from air exposure by Ar gas blowing during transferring to the sample chamber. High resolution transmission electron microscopy (HRTEM) observations were performed on Tecnai G2 F30 S-Twin, Philips-FEI.

3. Results

3.1. LaB_6 synthesis through reaction of $LiBH_4$ with $La(OH)_3$ or La_2O_3

After ball milling of $6LiBH_4 + La(OH)_3$ at 400 rpm for 16 h, the mixture was transferred into a reactor under Ar atmosphere in a glovebox. Fig. 1 shows hydrogen release of the mixture during heating from room temperature to 600 °C, which is obtained by assuming that the emitted gas was only hydrogen. Two stages of

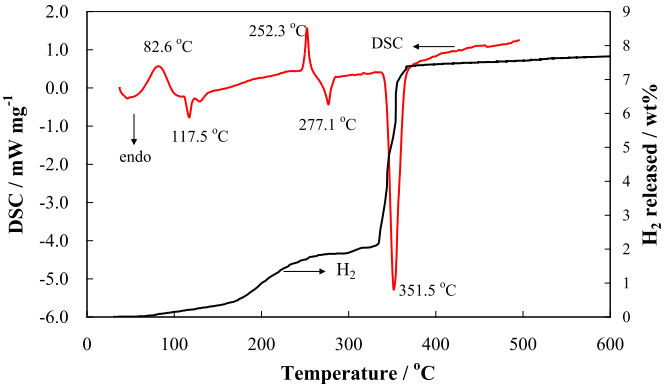

Fig. 1. DSC curve and hydrogen release behavior during heating the ball milled mixture of $6LiBH_4 + La(OH)_3$.

hydrogen release can be observed in Fig. 1: it first started at about 70 °C and then speeded up at around 170 °C, but paused at 260 °C. Then at around 350 °C, a large amount of hydrogen was released significantly within a narrow temperature range, implying a fast reaction. After this reaction, almost no hydrogen gas was further emitted even though the reactor was subsequently heated to 600 °C.

The DSC curve of the sample heated from room temperature to 500 °C is also presented in Fig. 1. During heating, two small exothermic peaks were observed at 82.6 °C and 252.3 °C respectively. Also two endothermic peaks at 117.5 °C and 277.1 °C were detected, which are close to the structural change and the melting temperatures of $LiBH_4$. These two endothermic peaks are weak compared to those of pure $LiBH_4$, implying that only a small amount of $LiBH_4$ was left at this stage. Then a large and sharp endothermic peak appeared at 351.5 °C, which is coincident with the significant hydrogen release at this temperature. Fig. 1 demonstrates that the reaction was accomplished within a very narrow temperature range and accompanied with a significant endothermic effect and considerable hydrogen release.

The *ex situ* XRD analysis results of the mixtures heated to different temperatures are shown in Fig. 2. Several new phases such as $LiBO_2$, La_2O_3 and $B_{20}H_{26}O$ were detected in the ball milled mixture, indicating that some reactions occurred during the ball milling treatment. Both La_2O_3 and $B_{20}H_{26}O$ seemed to remain until 300 °C while $LiBO_2$ was transformed. However, all these phases were not detected anymore in the sample heated to 400 °C, suggesting that they were only intermediates. Perfect diffraction patterns of LaB_6 were exhibited by the samples heated to 400, 500 and 600 °C, as shown in Fig. 2. In comparison, only extremely weak peaks of other substances such as Li_2O were detected in these samples. Based on the results shown in Figs. 1 and 2, it can be deduced that the significant reaction at 351.5 °C produced crystalline LaB_6. The further heating to 600 °C only induced slight growth of LaB_6 grains because the XRD peaks became somewhat stronger and narrower at higher temperatures. According to the Scherrer equation, the crystallite sizes of LaB_6 were calculated to be 23.3, 23.5, 26.0 nm at 400, 500 and 600 °C respectively. The cell parameters of LaB_6 obtained at 400, 500 and 600 °C were a = 4.1525, 4.1531 and 4.1443 Å, slightly smaller than the value of a = 4.157 Å given in the JCPDS card (PDF #65-1831).

The SEM photos in Fig. 3 demonstrate the morphologies of the products at three temperatures. Nearly spherical particles with a homogeneous size of less than 100 nm were achieved in all the samples. As shown in Fig. 3, only slight particle growth occurred in the samples with the increase of the temperature, which is in

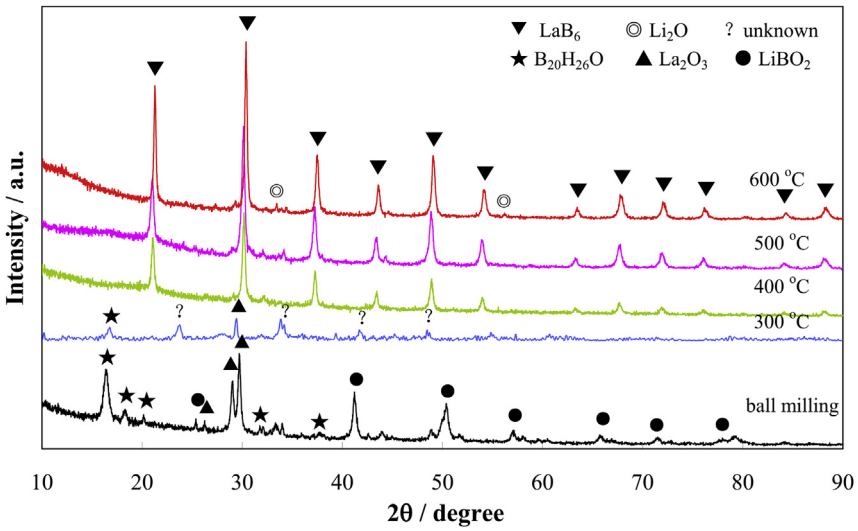

Fig. 2. XRD patterns of the $6LiBH_4 + La(OH)_3$ mixture at different reaction stages.

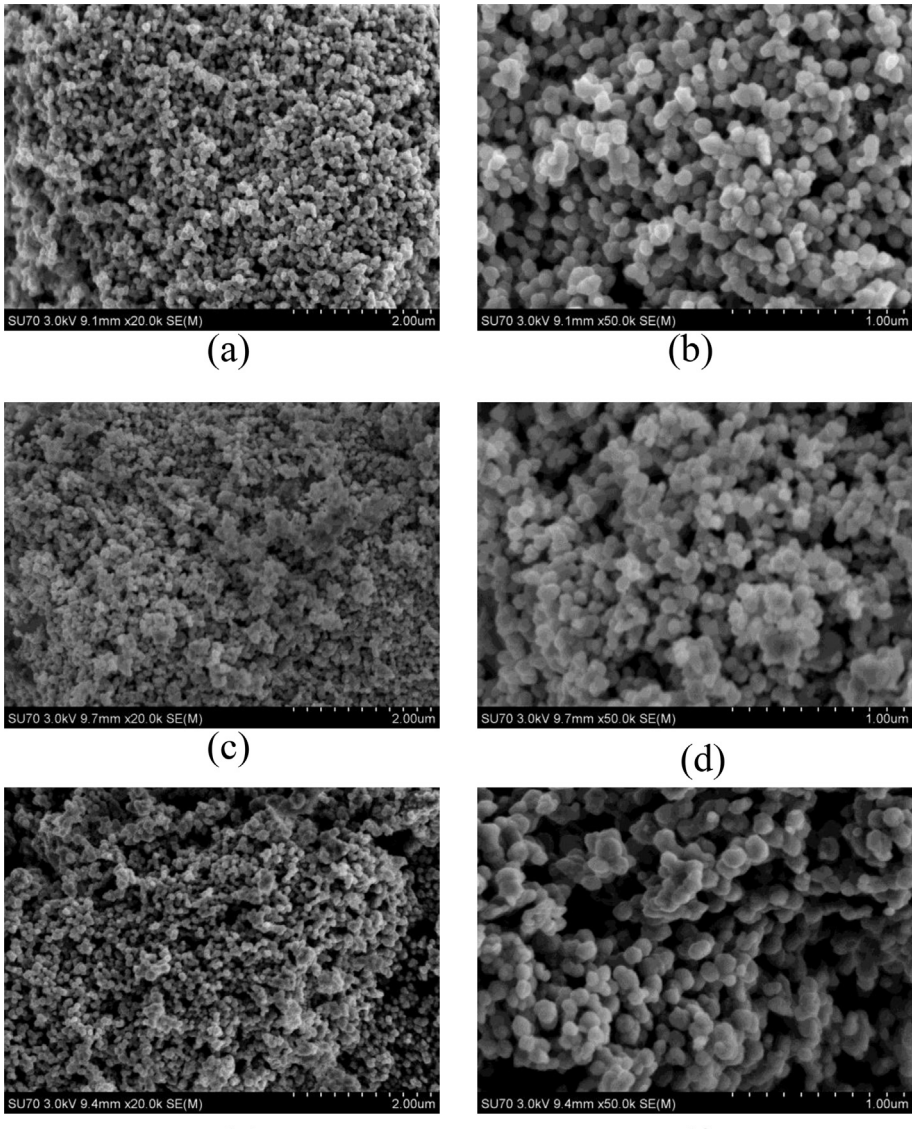

Fig. 3. SEM photos of the reaction products for $6LiBH_4 + La(OH)_3$ heated to 400 °C, 500 °C and 600 °C respectively. (a) and (b): 400 °C; (c) and (d): 500 °C; (e) and (f): 600 °C.

agreement with the XRD results.

The HRTEM observation shown in Fig. 4 reveals more clearly the morphology and structure of the formed LaB_6 nanoparticles. In Fig. 4(a), spherical particles smaller than 100 nm with a low degree of aggregation are well observed. Moreover, most of these particles are single crystals as shown by Fig. 4(b and d). The selected area electron diffraction (SAED) pattern shown in Fig. 4(d) reveals that the particle shown in Fig. 4(c) is a single crystal of LaB_6.

For comparison, La_2O_3 instead of $La(OH)_3$ was also used as the precursor to synthesize LaB_6. As shown in Fig. 5, the ball milled mixture of $12LiBH_4 + La_2O_3$ had a significant reaction at around 350 °C, resembling that of $6LiBH_4 + La(OH)_3$. Their differences in hydrogen release behavior were that $6LiBH_4 + La(OH)_3$ released more hydrogen below 350 °C, while $12LiBH_4 + La_2O_3$ still emitted hydrogen slightly at temperatures higher than 350 °C. The DSC curves of $12LiBH_4 + La_2O_3$ and $6LiBH_4 + La(OH)_3$ are similar to each other in that both of them show a significant endothermic effect at 356.6 and 351.1 °C respectively. The XRD result of $12LiBH_4 + La_2O_3$ heated to 600 °C displays a predominant pattern of LaB_6 with only minor peaks from Li_3BO_3 and LiOH. It suggests that both $12LiBH_4 + La_2O_3$ and $6LiBH_4 + La(OH)_3$ produced crystalline LaB_6 through a similar reaction route.

3.2. TiB_2 synthesis from $LiBH_4$ and TiO_2

Fig. 6 reveals the hydrogen release behavior of the ball milled $2LiBH_4 + TiO_2$ mixture. It can be seen that the release of hydrogen continued from 120 °C to 500 °C, suggesting that the reaction between $LiBH_4$ and TiO_2 proceeded within a wide temperature range. Probably due to the continuous reaction, the DSC curve shown in Fig. 6 demonstrates an overall endothermic effect during the whole heating process. One apparent endothermic peak at 128.5 °C, which is close to the structural change temperature of $LiBH_4$, was observed. In addition, two small and wide endothermic peaks at 267.1 °C and 289.4 °C respectively were also detected.

The results of XRD measurements shown in Fig. 7 clearly demonstrate a gradual transformation from TiO_2 to TiB_2. After ball milling, the mixture only exhibited the peaks of Anatase-TiO_2 without peaks from $LiBH_4$, most probably because $LiBH_4$ became amorphous during ball milling. After heating, some new phases including LiH appeared. Moreover, the peak strengths of these new phases decreased with the increase of temperature, suggesting that they are reaction intermediates. Inversely, the peaks from TiB_2 became apparent as the temperature was increased up to 500 °C. The broad peaks of TiB_2 also indicate its nanosized structure. The

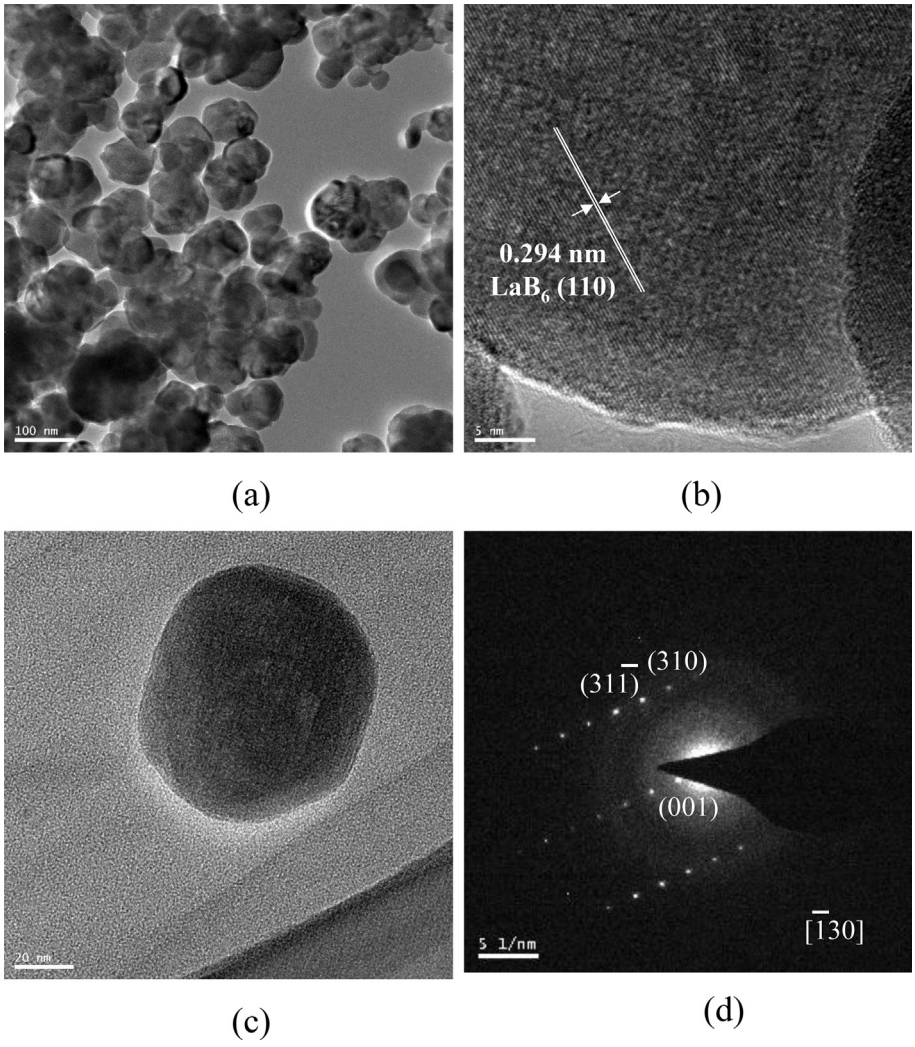

Fig. 4. HRTEM pictures of the reaction product for $6LiBH_4 + La(OH)_3$ heated to 600 °C. (a)–(c): morphologies of LaB_6 particles; (d) SAED pattern of the particle shown in (c).

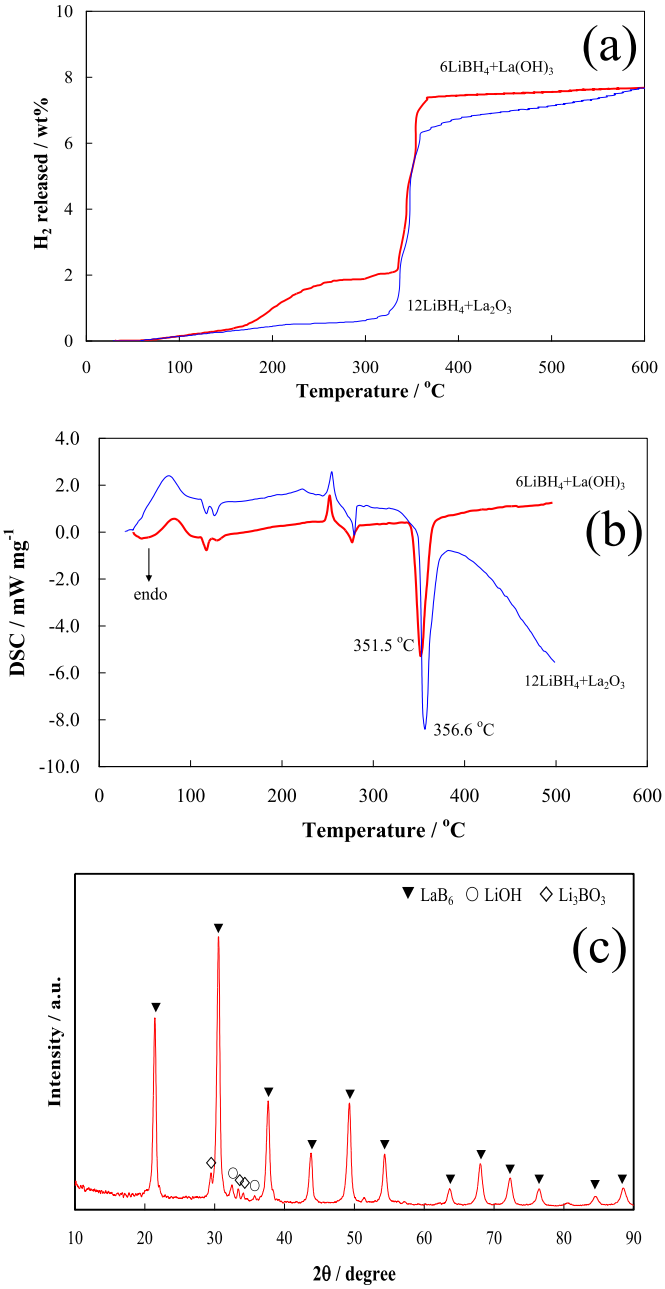

Fig. 5. Comparison between $12LiBH_4 + La_2O_3$ and $6LiBH_4 + La(OH)_3$. (a) hydrogen release behavior; (b) DSC curves; (C) XRD result of $12LiBH_4 + La_2O_3$ heated to 600 °C.

SEM and HRTEM pictures in Fig. 8 clearly display morphologies and nanostructures of the products at 400 °C and 600 °C respectively. Comparison of two SEM images reveals that the particles became more coalescent at 600 °C. From HRTEM pictures, nanocrystalline TiB_2 domains of only a few nanometers could be observed in the final product. However, it seems that the present reaction condition did not ensure a complete transformation from the intermediate into TiB_2. Higher temperature or longer reaction time is thus required.

4. Discussion

In this study, nanosized LaB_6 was successfully synthesized through reaction of $LiBH_4$ with $La(OH)_3$ or La_2O_3. The main reaction

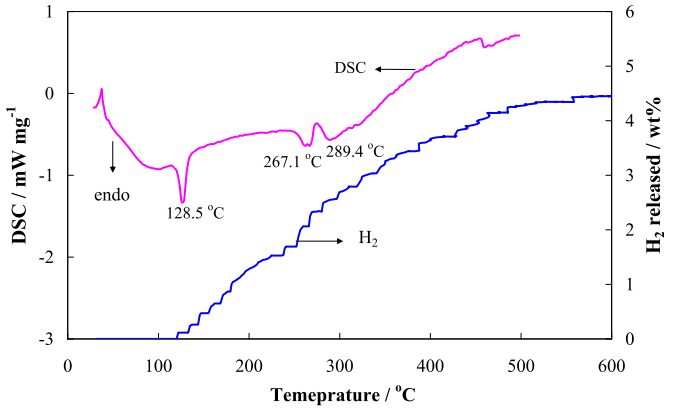

Fig. 6. DSC and hydrogen release curves of the ball milled $2LiBH_4 + TiO_2$ mixture.

occurred around 350 °C with a significant endothermic effect. The fast reaction resulted in a complete transformation into LaB_6 nanoparticles of good crystallinity. Also the low reaction temperature ensured a homogeneous nanosize of smaller than 100 nm.

Though there were compounds such as $LiBO_2$, La_2O_3, $B_{20}H_{26}O$ detected after ball milling or heating, it seems that they were only reaction intermediates because they were not present in the final products. As LaB_6 and Li_2O were detected in the final product, we thus suppose that the reaction can be written as follows:

$$6LiBH_4 + La(OH)_3 \rightarrow LaB_6 + 3Li_2O + 13.5H_2 \quad (1)$$

Based on the above equation, about 8.4 wt% hydrogen will be released with respect to the total weight of $6LiBH_4 + La(OH)_3$. In our experiment, about 7.8 wt% hydrogen was obtained, which is close to the value predicted by the reaction (1).

Both $12LiBH_4 + La_2O_3$ and $6LiBH_4 + La(OH)_3$ mixtures revealed the similar endothermic reaction at around 350 °C. It is thus supposed that they had analogous reaction pathway to produce crystalline LaB_6. However, the Li-containing by-products may be different for both mixtures in consideration of chemical balance. Determination of the exact side products other than LaB_6 for $12LiBH_4 + La_2O_3$ needs further research work.

As LaB_6 is not soluble in water, it is thus possible to separate it from other reaction by-products such as Li_2O or LiOH that are soluble in water. Therefore, pure LaB_6 can be achieved simply through water-washing the solid reaction product.

In contrast to a fast reaction occurring within a narrow temperature range for the mixture of $LiBH_4$ with $La(OH)_3$ or La_2O_3, the reaction of TiO_2 with $LiBH_4$ proceeded within a much wider temperature range from 120 °C to 500 °C. Based on the XRD results, the reaction is supposed to be as follows:

$$2LiBH_4 + TiO_2 \rightarrow TiB_2 + 2LiOH + 3H_2 \quad (2)$$

In the above equation, LiOH is deduced as a product mainly based on the chemical balance though it was not directly detected. According to the above equation, 4.9 wt% hydrogen will be released during the reaction. About 4.5 wt% hydrogen was actually obtained in our experiment, thus partially confirming the above reaction mechanism.

The slow and gradual reaction between $LiBH_4$ and TiO_2 is beneficial for the formation of nanosized TiB_2. However, it also hinders the complete transformation into TiB_2, thus decreasing the conversion efficiency. As $LiBH_4$ or LiOH is soluble in water, it is easy to separate them from Ti-containing compounds through water washing. But if the Ti-containing intermediate is not completely

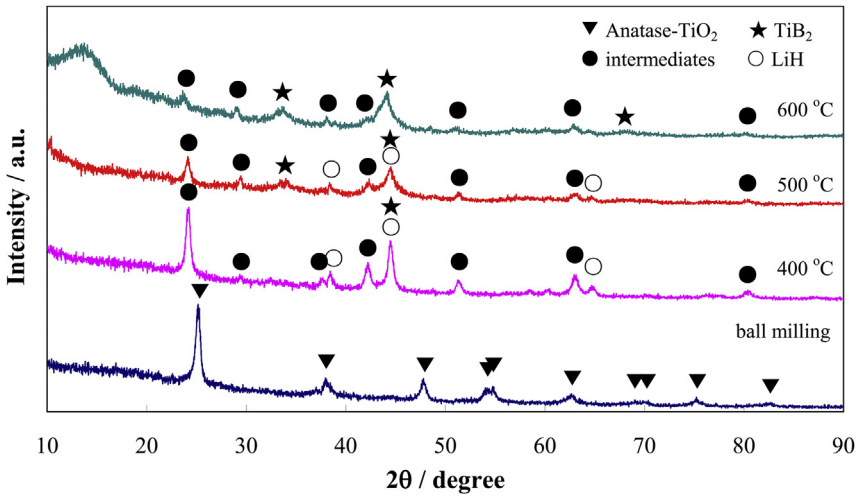

Fig. 7. XRD patterns of the $2LiBH_4 + TiO_2$ mixture heated to different temperatures.

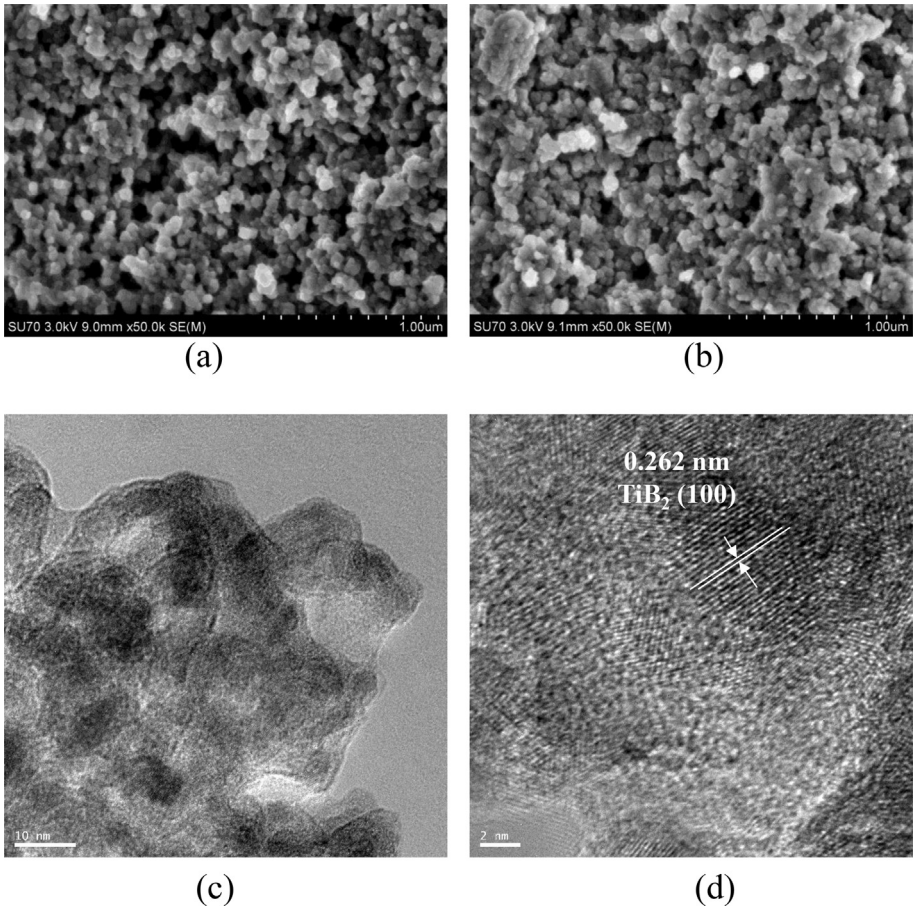

Fig. 8. SEM and HRTEM photos of the reaction product for $2LiBH_4 + TiO_2$. (a): SEM, heated to 400 °C; (b): SEM, heated to 600 °C; (c) and (d): HRTEM, heated to 600 °C.

transformed into TiB_2, it would be difficult to separate it from TiB_2. Therefore, it is highly required to achieve complete transformation through optimizing reaction conditions.

In our experiment, we found that the reaction of $LiBH_4$ with oxides or hydroxides can be extended to synthesize other transition metal borides. For example, this method may also be applied to the synthesis of other rare earth metal hexaborides such as CeB_6. We also successfully fabricated nanosized ZrB_2 through reaction of $LiBH_4$ with ZrO_2 below 600 °C. However, borides of main group metals such as MgB_2 could not be obtained by heating the ball milled mixture of $2LiBH_4 + MgO$. In this case, the self-decomposition of $LiBH_4$ occurred while MgO remained unreacted.

Compared with previously reported synthetic routes of metal borides, the present synthesis method is superior to the others in

following aspects: First, $LiBH_4$ was employed as the reactive boron source as well as the reductive agent, thus initiating the reaction at lower temperatures. Also its low melting temperature of 288 °C enabled the reaction to proceed in liquid–solid states that would enhance the reaction kinetics. Second, metal hydroxides or oxides instead of metal halides were used as the precursors in this study, resulting in endothermic synthetic reactions of metal borides. This is the main distinction between the present method and the others reported previously. Most of the reported synthetic reactions for metal borides are exothermic, thus suffering from poor control of reaction temperature and then particle size [1]. In comparison, the endothermic nature of the synthesis reactions presented in this study allowed for a precise control of reaction temperature and the resulting nanostructures including crystallinity, particle shape and size. Third, the synthesis method used in this study proved to be a facile and general route to fabricate nanosized transition metal borides including MB_2 and MB_6 structures under mild conditions. It is easy to achieve not only individual metal borides but also their composites in nanosizes through this method. For example, we have successfully synthesized a composite of LaB_6 and ZrB_2 through simple one-pot reaction, which is an important boride composite for high temperature applications.

5. Conclusions

In this work, nanosized transition metal borides such as LaB_6 and TiB_2 were successfully synthesized through reaction of $LiBH_4$ with the corresponding hydroxides or oxides at temperatures below 600 °C. In the ball milled mixture of $6LiBH_4 + La(OH)_3$ or $12LiBH_4 + La_2O_3$, a fast endothermic reaction at around 350 °C produced crystalline LaB_6 nanoparticles of a size smaller than 100 nm. Though some intermediates were formed during the reaction, LaB_6 was found as the only boride in the reaction product and can be easily separated from other water soluble side products. In comparison, the reaction of $LiBH_4$ and TiO_2 took place within a wide temperature range from 120 °C to 500 °C. The slow and gradual reaction produced TiB_2 nanoparticles of only a few nanometers. The successful synthesis of these borides suggests that this approach is a facile and general synthesis route for transition metal borides.

Acknowledgments

This work is financially supported by the National Natural Science Foundation of China under grant Nos. 51271164, 21276229 and 21476200.

References

[1] S. Carenco, D. Portehault, C. Boissiere, N. Mezailles, C. Sanchez, Chem. Rev. 113 (2013) 7981–8065.
[2] B. Albert, H. Hillebrecht, Angew. Chem. Int. Ed. 48 (2009) 8640–8668.
[3] J. Stuart, A. Hohenadel, X. Li, H. Xiao, J. Parkey, C.P. Rhodes, S. Licht, J. Electrochem. Soc. 162 (2015) A192–A197.
[4] J. Stuart, M. Lefler, C.P. Rhodes, S. Licht, J. Electrochem. Soc. 162 (2015) A432–A436.
[5] Z. Huang, R. Lin, R. Fan, Q. Fan, J. Ma, Electrochim. Acta. 139 (2014) 48–53.
[6] J. Liu, S. He, C. Li, F. Wang, M. Wei, D.G. Evans, X. D, J. Mater. Chem. A 2 (2014) 7570–7577.
[7] B.H. Liu, Q. Li, Int. J. Hydrog. Energy 33 (2008) 7385–7391.
[8] S. Rades, S. Kraemer, R. Seshadri, B. Albert, Chem. Mater. 26 (2014) 1549–1552.
[9] D. Portehault, S. Devi, P. Beaunier, C. Gervais, C. Giordano, C. Sanchez, M. Antonietti, Angew. Chem. Int. Ed. 50 (2011) 3262–3265.
[10] J.W. Kim, J.H. Shim, J.P. Ahn, Y.W. Cho, J.H. Kim, K.H. Oh, Mater. Lett. 62 (2008) 2461–2464.
[11] Y. Yan, Z. Huang, S. Dong, D. Jiang, J. Am. Ceram. Soc. 89 (2006) 3585–3588.
[12] H.E. Camurlu, F. Maglia, J. Eur. Ceram. Soc. 29 (2009) 1501–1506.
[13] D. Lee, G.D. Sim, K. Xiao, J.J. Vlassak, J. Phys. Chem. C 118 (2014) 21192–21198.
[14] M. Zhang, L. Yuan, X. Wang, H. Fan, X. Wang, X. Wu, H. Wang, Y. Qian, J. Solid State Chem. 181 (2008) 294–297.
[15] L. Wang, L. Xu, Z. Ju, Y. Qian, CrystEngComm 12 (2010) 3923–3928.
[16] J.P. Kelly, R. Kanakala, O.A. Graeve, J. Am. Ceram. Soc. 93 (2010) 3035–3038.